Cadaveric Simulation of Flatfoot and Surgical Corrective Techniques: The Evans versus the Z-osteotomy

Grant C. Roush

A thesis
submitted in partial fulfillment of the
requirements for the degree of

Master of Science in Engineering

University of Washington

2013

Committee:
William R. Ledoux
Randal P. Ching
Nathan J. Sniadecki

Program Authorized to Offer Degree:

Department of Mechanical Engineering

Table of Contents

List of Figures

List of Tables

Abstract

The main clinical purpose of this study is to compare two different surgical procedures, the Evans calcaneal osteotomy and the Z-osteotomy, both of which are used to correct Stage II (flexible) cases of flatfoot deformity. This work is a follow-up to a pilot study completed previously by the VA Center of Excellence for Limb Loss Prevention and Prosthetic Engineering (VA RR&D). In that study, the feet (both flat and corrected) were statically placed at mid-stance of the gait cycle and data were collected. Kinematic and kinetic comparisons were made to see how each surgery performed in restoring the foot to normal shape and function. This research looks to build on that study by using a fully dynamic *in vitro* simulation of the stance phase of gait.

A process of ligament attenuation coupled with axial loading of the foot has been developed by our group to induce a flexible flatfoot on neutrally aligned cadaveric specimens. Previous research has shown the ligaments most involved in supporting the medial arch were the superomedial and inferomedial calcaneonavicular (spring), talocalcaneal interosseous, plantar naviculocuneiform, plantar first metatarsocuneiform, and anterior superficial deltoid ligaments. To induce weakening in our study, these ligaments were either sectioned or attenuated with multiple longitudinal incisions parallel to the fiber orientation, after which the foot was cyclically loaded from 10 N to body weight at 2 Hz until visual evidence of flatfoot was seen. In addition, X-rays were taken and clinical measurements were performed to assess foot shape initially, after the flattening procedure, and post-surgery. The repeatability of making these measures was also investigated.

Gait simulation was performed with the robotic gait simulator (RGS) at the VA RR&D. The RGS was developed to allow for *in vitro* simulation of the stance phase of gait using

cadaveric specimens. It has been shown to accurately simulate both the kinematics and kinetics of the foot during the stance phase of gait. Having a physiologically correct model will allow for the most accurate representation of *in vivo* gait currently possible, while also allowing the utilization of invasive measurement techniques (such as insertion of bone pins) or multiple surgical procedures that would otherwise be impossible on living human subjects.

Results from this work have shown that our flatfoot model has the ability to create a mild Stage II flatfoot deformity in previously neutrally aligned cadaveric specimens. Additionally, evidence proved our process for collecting and measuring clinically relevant radiographic measures was highly repeatable. Both static radiographic evidence and dynamic simulation showed significant differences after lateral column lengthening, most notably an increase in lateral peak plantar pressures post-surgery, but there were few differences when comparing the two surgical procedures.

Chapter 1: Introduction

Flatfoot (pes planus) is one of the most common foot conditions affecting patients of all demographics in the U.S.[1] Often pes planus has a musculotendonous component (e.g., posterior tibial tendon deficiency (PTTD), which can be exacerbated by circulatory deficiencies (e.g., diabetes), and/or increased loading due to obesity. Flatfoot presents itself with a collapse of the medial longitudinal arch of the foot, which is often accompanied by hindfoot valgus and forefoot abduction (Figure 1.1).[2] There is no standardized method for treating flatfoot, and various techniques to abate symptoms can include orthoses, immobilization and, in cases where conservative treatment fails, surgical correction. These corrective surgeries may include combinations of the following: tendon transfers or lengthenings, medial column plantar flexor osteotomies, medial column stabilizations, various hindfoot osteotomies and/or hindfoot arthodeses. Of note is that there is little agreement among surgeons as to which surgical procedures to perform and that the most common hindfoot osteotomy procedures (the medializing calcaneal osteotomy (MCO),[3] the Evans calcaneal osteotomy,[4] and the calcaneocuboid distraction arthrodesis (CCDA)[5]) can all lead to increased lateral forefoot pressure. More recently, a calcaneal Z-osteotomy is being used clinically to treat severely deformed, flexible flatfoot;[6] however, this procedure has not been objectively studied.

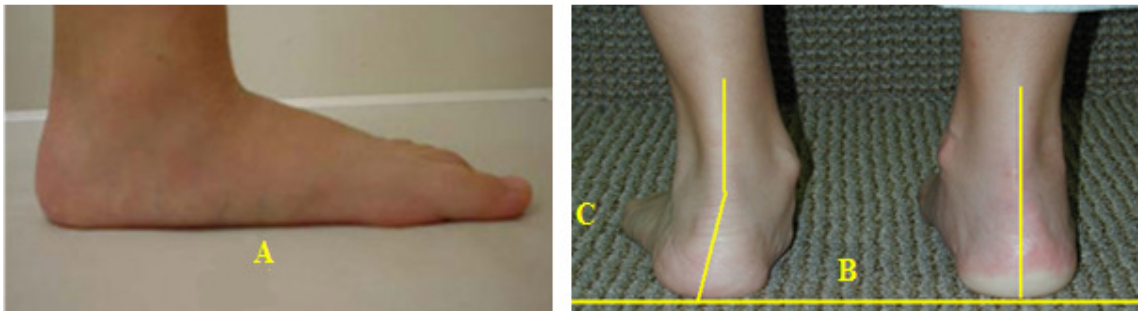

Figure 1.1: External clinical symptoms of flatfoot: A) collapse of the medial arch, B) hindfoot valgus, and C) forefoot abduction (presenting with 'too many toes' sign).

There are various avenues for studying the flatfoot deformity and possible surgical corrections. Examining human subjects is one option, but *in vivo* studies can be time consuming and expensive, and are limited to measurements that can be made without harming the patient. Additionally, it can be difficult to make direct comparisons between differing medical procedures based on the number of confounding variables that arise from patient-specific treatments. Computer models are also potentially powerful tools, but they are limited to some degree by the robustness of their creation and the rigorousness of their validation. Issues such as anatomical accuracy, tissue mechanical properties and biofidelic boundary conditions are all critical. Cadaveric models, whereby *in vitro* lower limbs are loaded in physiological simulations, are useful tools that have often been used to explore more invasive foot biomechanics.[7,8] They provide a mechanism for quantitatively exploring foot mechanics and various treatment strategies. They allow for the measurement of parameters that would not be ethically possible with living humans (e.g., motion quantified with bone pins). Many studies involving flatfoot in cadaveric specimens have been performed, but due to the limitations of working with cadavers, most of these studies are either static or quasi-static, and investigate the foot at midstance,[9] or at a select few locations within stance.[10] More recently, dynamic gait simulators have been developed that allow researchers to conduct fully dynamic simulations using cadaveric specimens.[11] This allows for the ability to simulate and analyze the entire stance phase of gait. To date, there is limited investigation into the biomechanics of flatfoot using this technology.

Current methods used in creating cadaveric flatfoot models from neutrally aligned feet include either substantial sectioning of ligaments[3] and/or tendons or surgical attenuation of selected ligaments and/or tendons followed by cyclic axial loading.[9,10] Sectioning simulates complete rupture, which does not occur in physiologic pes planus. Additionally, sectioning

important ligaments such as the plantar aponeurosis (PA) could lead to unrepresentative biomechanical response during dynamic gait simulations due to the importance of the PA as part of the windlass mechanism. Attenuation followed by cyclic axial loading is thought to simulate progressive development of soft tissue laxity in a more physiologic manner, and there is evidence that the medial ligaments of the foot become attenuated during the development of flatfoot.[12]

In order to accurately diagnose and/or quantify abnormalities in cadaver specimens, researchers must be able to reproduce clinical X-ray procedures which often require the foot to be in a load bearing position. While numerous studies exist for capturing and measuring diagnostic radiographs *in vivo*, to our knowledge, there is no study that investigates the accuracy and repeatability of collecting and analyzing cadaver radiographs.

Previous work in our lab involved the development of a robotic gait simulator (RGS) that has proven to be a valuable research tool, as it allows for simulation of the entire stance phase using advanced control mechanisms to accurately recreate desired vertical ground reaction force profiles using physiologic inputs (tibial kinematics, muscle force profiles, etc.).[11] Based upon the lack of research that has been done studying the Z-osteotomy procedure, and the limited validation of cadaveric radiographic screening, this work looks to add to flatfoot research by:

1.) Developing a system of gathering clinical, load-bearing radiographs of cadaveric specimens, and assessing the repeatability of common bony measurements that quantify foot shape (Ch. 2).
2.) Developing a cadaveric flatfoot model that is as similar to physiologic conditions as possible by using evidence-based ligament attenuation followed by cyclic axial

compression with tendons loaded, rather than just sectioning. We believe that this will better simulate the physiologic conditions that lead to the flatfoot (Ch. 3).

3.) Comparing and contrasting the well-established Evans osteotomy with the Z-osteotomy by studying surgical correction outcomes radiographically, and using the RGS to investigate kinematic and kinetic changes that occur after correction (Ch. 3).

Additionally, during test planning, a question arose as to how kinematics of the tibia may be affected by foot shape. To accurately simulate gait using cadaver feet, the motion of the tibia with respect to the ground is often employed; thus, so it is important to know if tibial kinematics differ significantly between foot type. Therefore, a secondary and collaborative study was undertaken to investigate the effect of foot type on tibial kinematics (Appendix A).

Chapter 2: Clinical Foot and Ankle X-rays with Cadaveric Specimens

ABSTRACT

Background: Advances in the dynamic simulation of the stance phase of gait using cadaveric feet have provided a new avenue to gain a better understanding of foot morphology and biomechanics. The simulation of pathologic foot disorders and related corrective surgical procedures requires a repeatable way to assess foot shape. A common clinical tool to assess foot type and diagnose abnormalities is the measurement of bone-to-bone position in multi-planar X-rays. While numerous studies exist for capturing and measuring diagnostic X-rays *in vivo*, the novel contribution of our study is the investigation of the repeatability of cadaveric X-ray measures.

Materials and Methods: Eight fresh-frozen human cadaveric feet were used to study five common X-ray measurements. To test the repeatability of our custom loading apparatus, three feet were loaded and X-rayed three times each and measured by one rater. The remaining five feet were X-rayed and measured five times each by two raters. The variability and inter- and intra-rater correlation coefficients (ICCs) were determined for all measures.

Results: All ICCs were greater than 0.8, with 11 of 15 greater than 0.94, demonstrating excellent measurement repeatability. Loading and positioning the foot within the apparatus does not significantly alter the X-ray measurements. For inter- and intra-rater variability, the navicular height was the most repeatable measurement, while the talonavicular coverage angle was the least.

Conclusion: This study demonstrates that our loading technique and measurement methods are repeatable for collecting clinically relevant foot and ankle X-rays using cadaveric specimens.

INTRODUCTION

Cadaveric research has played a vital role in the current understanding of foot morphology and biomechanics. Dynamic gait simulation[11] has shed new light on foot function and allowed for invasive access to individual foot bones[7] that could not easily be studied *in vivo*. Additionally, pathologies can be simulated in these feet in order to better understand abnormalities and the surgical procedures used to correct them. However, in order to accurately identify foot bone position in both normal and pathologic cadaveric specimens, researchers must be able to reproduce clinical X-rays, which often require the foot to be weightbearing.

Assessment of foot shape can be performed using three X-ray views: anterior/posterior (AP), medial/lateral (ML), and hindfoot alignment. From these three views, a number of bony measurements can be made in order to assess the overall alignment of the foot, a combination of which is frequently used to assess foot type. Such measurements include: from the ML view - calcaneal pitch (CP), lateral talometatarsal angle (LTMA), and navicular height (NH); from the AP view - talonavicular coverage angle (TNCA); and from the hindfoot view - calcaneal eversion distance (CED). Due to the importance of properly identifying foot type and other abnormalities, it is imperative that repeatable measurements are made. Numerous *in vivo* studies exist that address inter- and intra-rater repeatability of radiographic measurements.[4,13-17] There are also studies that utilize radiographic measurements to assess foot shape in cadaveric specimens,[5,18] but to our knowledge, there is no study that investigates the repeatability of collecting and analyzing cadaveric radiographs. The purpose of this study was to assess the repeatability of common measurements from weight-bearing cadaveric foot X-rays.

Materials and Methods

Eight fresh-frozen cadaveric feet (mean age 77.9 ± 15 years, range 51 to 93 years; six female, two male) with no visible mid- or hindfoot pathologies were chosen for this study. X-rays were taken using a custom loading apparatus (Figure 2.1) and a Faxitron X-ray cabinet and digital scanner (Faxitron, Tucson, AZ). Each foot was loaded to 25% of the specimen's body weight (BW) through the tibia only using a calibrated compressed spring; the scaled BW was selected primarily because planned gait simulations also used a scaled BW due to limitations of loading fragile cadaveric specimens. The apparatus was oriented in the X-ray cabinet to allow for the AP, ML and hindfoot alignment views (Figure 2.2). The following five measurements were made to quantify foot bone: CP,[19] LTMA,[19] and NH (similar to medial column height from Ellis[4]) to quantify arch height; TNCA[19] to quantify forefoot abduction/adduction; and CED[15] to quantify hindfoot inversion/eversion.

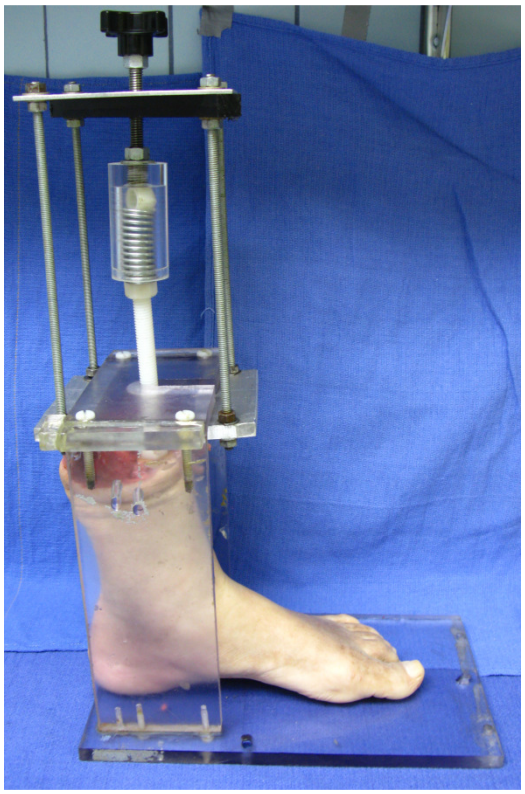

Figure 2.1: Foot in X-ray apparatus with load applied through a compressed spring.

To test the repeatability of loading the foot into the apparatus, three of the feet were loaded three times each and all X-rays were collected and measured by a single experienced rater. To test the inter- and intra-rater repeatability of the measurements, the remaining five feet were loaded and all X-rays were obtained. These feet had undergone a flattening procedure[9] as part of a coincident study.[20] The resulting 15 X-rays were then blinded and measured by two experienced raters five times each in a randomized order, for a total of 75 measured X-rays per rater. All length measurements used a scaling factor to account for radiographic magnification effects. Each of the five sets was examined with three to five days between measurements.

Linear mixed effects regression was used to determine standard deviation (SD) and the inter- and intra-class correlation coefficients (ICC) for the loading and measurement repeatability. Results were grouped using the following common classification scheme for ICCs: < 0.40 = poor, 0.40 - 0.74 = fair to good, and > 0.74 = excellent.[21]

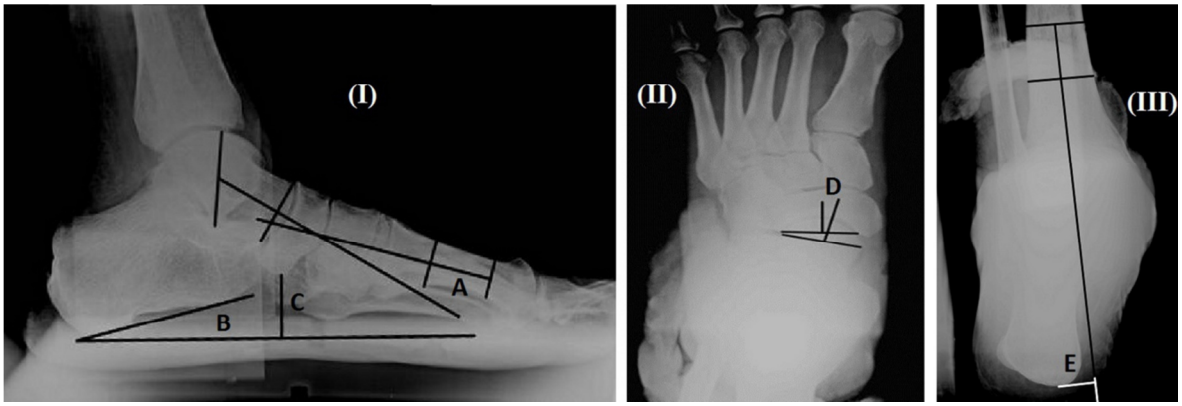

Figure 2.2: (I) Medial-lateral [ML] X-ray view with the (A) lateral talometatarsal angle [LTMA], (B) calcaneal pitch [CP], and (C) navicular height [NH] measurements shown; (II) Anterior-posterior [AP] X-ray view with the (D) talonavicular coverage angle [TNCA]; (III) Hindfoot alignment X-ray view with the (E) calcaneal eversion distance [CED].

Results

Overall, there was excellent repeatability for both the loading and measurement methods, with all ICCs greater than 0.8, and 11 of 15 greater than 0.94 (Table 2.1). From the loading repeatability data, TNCA (ICC value of 0.98), CP (0.98), and CED (0.97) were least affected by

the multiple loads, while NH (0.82) and LTMA (0.83) were slightly more variable between loading trials. For both the inter-rater and intra-rater measurement repeatability, NH (0.99 and 0.98, respectively) proved to be the most repeatable, while the TNCA (0.80 and 0.82, respectively) was the least repeatable.

Table 2.1: Standard deviation and ICCs for the loading variability, as well as inter-rater and intra-rater variability.

	Loading variability		Inter-rater variability		Intra-rater variability	
	SD	ICC	SD	ICC	SD	ICC
CP (degrees)	0.57	0.98	0.01	0.94	0.73	0.94
LTMA (degrees)	1.6	0.83	<.0001	0.96	1.6	0.96
NH (mm)	0.15	0.82	<.0001	0.99	0.48	0.98
TNCA (degrees)	1.6	0.98	0.40	0.80	3.0	0.82
CED (mm)	1.7	0.97	<.0001	0.94	1.4	0.94

Discussion

To better understand normal and abnormal foot function using cadaveric specimens, researchers will often attempt to induce pathologies, such as flatfoot, on neutrally aligned feet. [9,10,22] In order to ensure desired foot types have been simulated, clinical X-ray measurements are a useful means to quantify foot shape and changes in foot shape resulting from the application of biomechanical processes. Hence, a repeatable method to collect and measure X-ray images from cadaveric specimens is needed.

This study demonstrates that our method for loading cadaveric feet to 25% BW led to highly repeatable measurements. In general, measurements that were made from the ML view tended to have slightly greater variability between load applications, likely due to the fact that sagittal plane kinematics are more affected by loading through the tibia than the other cardinal planes. Previous studies show that well-established positioning techniques[15,17] for 50% BW *in vivo* foot X-rays produce repeatable measurements. The use of the calibrated compressed spring

loading method (which has some inherent variability) in this study, in conjunction with repeatable results, indicates that the X-ray measurements are not sensitive to applied loads near 25% BW. In a clinical setting, this may be beneficial for injured patients who can only tolerate a partial weight-bearing X-ray.

This study also demonstrates that our methods for measuring cadaveric foot X-rays are highly repeatable. In most cases, the inter-rater repeatability of our measurements closely matched or exceeded those from similar *in vivo* studies (Table 2.2).[4,13-16] ICC ranges of 0.76 to 0.95 were reported for the inter-rater repeatability of the CP measurement. For the LTMA, the inter-rater ICC range was 0.78 to 0.83, and though no study directly reported repeatability of NH, a similar measure of the medial column height showed an ICC range of 0.90 to 0.93. For the AP X-ray, *in vivo* measurement of the TNCA showed less repeatability between raters with an ICC range of 0.30 to 0.91. The reported values for CED also showed large variability of ICC measurements ranging from 0.51 to 0.96.

Table 2.2: A comparison of ICC values from our study to those found in similar *in vivo* studies.

Inter-rater reliabilities

Study	CP	LTMA	NH	TNCA	CED
In vitro	0.94	0.96	0.99	0.80	0.94
In vivo	0.76 - 0.95[a,b,d,e]	0.78 - 0.83[a,b,d,e]	0.90 - 0.93♠[a,e]	0.30 - 0.91[a,b,e]	0.51 - 0.96[a,c,d]

Intra-rater reliabilities

Study	CP	LTMA	NH	TNCA	CED
In vitro	0.94	0.96	0.98	0.82	0.94
In vivo	0.68 - 0.98[b,d,e]	0.75 - 0.93[b,d,e]	0.51♠[e]	0.01 - 0.95[b,e]	0.89 - 0.95[d]

(♠) Similar measure of medial column height
a.) ref. 4 b.) ref. 16 c.) ref. 15 d.) ref. 13 e.) ref. 14

Intra-rater repeatability was also excellent for all X-ray measures, matching or exceeding that of *in vivo* studies (Table 2.2). ICC ranges of 0.68 to 0.98 were reported for the intra-rater repeatability of the CP. For the LTMA, the intra-rater ICC range was 0.75 to 0.93, and the medial column height showed an ICC of 0.51 *in vivo*. For the AP X-ray, *in vivo* measurement of the TNCA showed the most variability in measurements with an ICC range of 0.01 to 0.95 reported. The reported values for CED showed ICC measurements ranging from 0.89 to 0.95.

Possible limitations in this study include the scaled body weight (25%), which could lead to more conservative X-ray measurements than would be seen in higher load bearing clinical X-rays. However, it should be acknowledged that 50% body weight is typically applied during *in vivo* X-rays. Also, loading was concentrated through the tibia, whereas *in vivo* X-rays include fibular loading as well. For the loading repeatability, slight misalignments of the foot position in the apparatus or the apparatus position in the X-ray cabinet between loading trials were not accounted for; however, attempts were made to be repeatable with positioning, and high measurement ICC values indicated a low sensitivity to possible misalignments. Furthermore, the cadaveric foot tissue could also potentially creep while the foot was in the apparatus. Additionally, no muscle forces were simulated during the X-rays. Finally, although our measurements and loading techniques were highly repeatable, there was no attempt in this study to validate the accuracy of the selected points.

This study demonstrates that our loading technique and measurement methods are repeatable for collecting clinically relevant foot and ankle X-rays using cadaveric specimens. Similar, or better, results were found compared to *in vivo* studies, demonstrating that our *in vitro* methods are at least as repeatable.

Chapter 3: Cadaveric Simulation of Flatfoot and Surgical Corrective Techniques: the Evans Versus the Z-Osteotomy

Abstract

***Background*:** Symptomatic flatfoot (pes planus) is a common foot condition that is often treated with lateral column lengthening (LCL) procedures such as the Evans LCL. More recently, the Z-osteotomy has been proposed as an alternative to the Evans. The purpose of this study is to compare the surgeries both statically using radiographs and dynamically using our robotic gait simulator (RGS).

***Methods*:** Flatfoot was produced in cadaveric specimens by attenuating the ligaments that support the medial arch and cyclically loading through the tibia to weaken the structures. Common diagnostic measures from clinical X-rays were used to assess foot shape. Each flatfoot was then tested on the RGS with ground reaction forces scaled to 25% of the donor's body weight and the stance phase simulated 6x slower than physiologic gait (4.09s). After flatfoot data collection, one foot in each pair received the Evans LCL while the other received the Z-osteotomy. Post-surgery X-rays were taken, and the feet were once again tested on the RGS. Kinematic and kinetic data were collected and compared for both flatfoot and post-surgical trials.

***Results*:** All X-ray parameters were significantly different after the flattening procedure indicating flattening of the arch, forefoot abduction, and hindfoot eversion. The calcaneal pitch angle decreased, though not to the level seen in physiologic flatfoot. Significant changes toward arch restoration were seen in the X-ray parameters after surgeries, but there were no radiographic differences between surgery type. Peak pressure under the lateral forefoot significantly increased after both surgeries, but did not differ between procedures. Finally, kinematic data only showed a few differences between the Evans and the Z-osteotomy.

***Conclusions*:** Radiographic evidence demonstrated that our model produced a mild Stage II flexible flatfoot from neutrally aligned cadaveric specimens, and post-surgical feet showed significant improvement. Few differences between the surgical techniques were seen in the kinematic and kinetic data.

***Clinical Relevance*:** This study found that the Evans and Z-osteotomies are similar in their ability to biomechanically address flatfoot.

Introduction

Symptomatic flatfoot (pes planus) is a common debilitating foot condition[1]. The onset of the adult acquired flatfoot can often be traced to posterior tibial tendon dysfunction (PTTD)[23,24]. Over time, patients with PTTD begin to see a collapse of the medial longitudinal arch of the foot, which is often accompanied by forefoot abduction and hindfoot valgus. These changes often lead to increased pain in the arch, abnormal gait patterns, and the need for clinical intervention.

Johnson and Strom[25] developed a method for classification of flatfoot into three stages, which was later extended into four by Myerson[2]. Stages I and II are characterized by pain, swelling, and a flexible hindfoot, with Stage II also including a valgus angulation of the heel and the inability to perform a single leg heel rise. The defining characteristic in Stage III and IV is a rigid hindfoot, with Stage IV including valgus angulation of the talus. Surgical correction is often employed in Stage II, and commonly includes a lateral column lengthening (LCL) procedure such as the Evans LCL[26] coupled with a soft tissue procedure such as a flexor digitorum longus transfer[27]. More recently, the Z-osteotomy[28] has been proposed as an alternative to the Evans[6]. The Z-osteotomy, also an LCL, has more bone-on-bone contact, which is thought to improve healing, and can be performed on flatfeet with a normal calcaneal pitch angle, a potential contra-indication of the Evans.

Numerous studies have investigated the *in vivo* etiology and radiographical diagnosis of flatfoot[14-16,19,29,30], while others have investigated biomechanical changes in the foot caused by the Evans procedure[4,31-33]. Ellis et al. have shown that subjects with lateral foot pain after receiving the Evans procedure had significantly increased lateral foot pressure compared to non-painful post-surgical patients[4]. The biomechanical effects of the Z-osteotomy have not been fully explored.

A limitation of *in vivo* studies is the inability to explore foot function and morphology using invasive measures. As such, biomechanists often use cadaveric specimens to gain better understanding of foot function and to compare differing medical treatments. Many cadaveric studies involving flatfoot have been performed[5,9,10,18,22,34,35]; however, these studies are not without limitations, as all were static or quasi-dynamic, and several of these studies created a flatfoot from neutrally aligned feet by completely sectioning the ligaments responsible for arch integrity. More recently, dynamic gait simulators have been developed that allow researchers to conduct dynamic simulations using cadavers[8,11,36-39]. This allows for simulation of the entire stance phase of gait. To date, there is limited investigation into the biomechanics of flatfoot using this technology, especially related to the surgical correction of flatfoot.

The aims of this study are to create and validate a physiologic flatfoot model, and then to compare the Evans anterior calcaneal LCL and the Z-osteotomy using dynamic gait simulation. We hypothesize that the Z-osteotomy will demonstrate similar corrective power (determined via static X-rays) and show similar or less lateral forefoot pressure than the Evans, which would make the Z-osteotomy a viable alternative to the Evans.

Methods

Fourteen fresh-frozen neutrally aligned cadaveric lower limb specimens (seven pairs) were used in this study, with each foot transected approximately 12cm proximal to the ankle joint. Prior to dissection and testing, feet were screened radiographically for abnormalities. All skin, subcutaneous tissue, muscle, and fascia 2cm proximal to the medial malleolus were removed, and the following extrinsic tendons were exposed: tibialis posterior (TP), tibialis anterior (TA), extensor hallucis longus (EHL), extensor digitorum longus (EDL), peroneus

longus (PL), peroneus brevis (PB), flexor digitorum longus (FDL), flexor hallucis longus (FHL), and Achilles.

Stage II flatfoot was simulated by attenuating or sectioning ligaments involved in pes planus[12]. Multiple longitudinal incisions parallel to the fiber orientation were made in the talocalcaneal interosseous, plantar naviculocuneiform, plantar first metatarsocuneiform, anterior superficial deltoid, and superomedial and inferomedial calcaneonavicular (spring) ligaments[9]. To further weaken the ligaments, a cyclic axial load was applied to the tibia of all specimens using an 858 Mini Bionix II System (MTS, Eden Prairie, MN) with a 40˚ wedge under the medial calcaneus to promote calcaneal eversion. The force-controlled actuator applied loads up to the body weight (BW) of the specimen, and each foot was cycled at 2 Hz up to 35,000 times. After the first three pairs of feet were tested, the spring ligaments were sectioned, rather than attenuated, before cycling in an attempt to increase flattening.

Assessment of foot shape was performed using three common radiological views: anterior/posterior (AP), medial/lateral (ML), and hindfoot alignment (Figure 1). Each foot was loaded to 25% of the specimen's BW in a custom loading device. The following diagnostic measures were analyzed: calcaneal pitch angle (CPA)[19], lateral talometatarsal angle (LMTA)[19], navicular height (NH)[40], talonavicular coverage angle (TNCA)[19], and calcaneal eversion distance (CED)[15]. X-rays were taken three times: before and after the flattening procedure, and after surgical correction. Previous work has shown that the X-ray measurements were repeatable[41]. Each foot was then tested on the robotic gait simulator (RGS), which has been described in detail elsewhere[11]. In brief, the RGS moved a force plate attached in series with a pressure plate (i.e., the ground) with inverse motion with respect to the fixed tibia (Figure 2). Stance phase simulations were performed in 4.09 seconds and scaled to 25% of the donor's BW. Tibia

kinematics and ground reaction forces (GRF) were prescribed from *in vivo* data from 10 symptomatic flatfoot subjects[42]. Muscle forces from the literature were applied to the nine extrinsic muscle tendons via linear actuators[11]. For the first three pairs of feet, force was applied to TP, but to more closely mimic PTTD, TP remained inactive for the final four pairs. Two additional pairs of feet had been used in a previous study that required FDL transection, thus no pre-surgical forces could be applied. Three data trials per condition were collected for analysis.

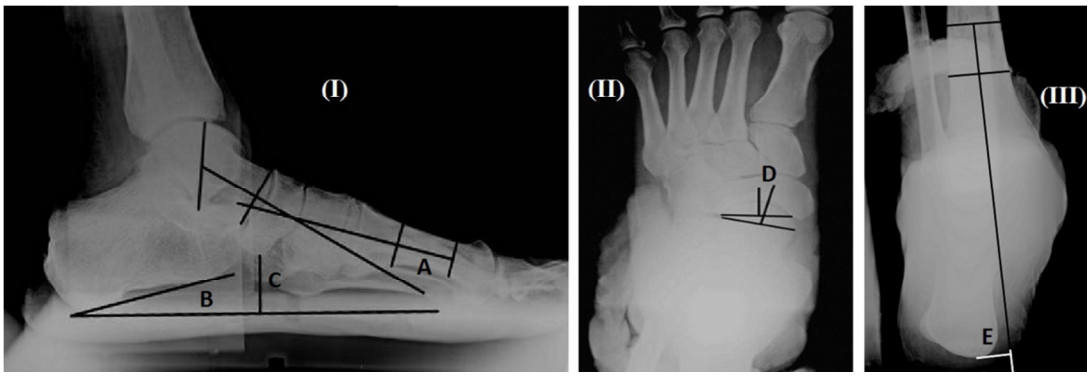

Figure 3.1: (I) Medial/lateral [ML] X-ray view with the (A) lateral talometatarsal angle [LTMA], (B) calcaneal pitch angle [CPA], and (C) navicular height [NH] measurements; (II) Anterior/posterior [AP] X-ray view with the (D) talonavicular coverage angle [TNCA] measurement; (III) Hindfoot alignment X-ray view with the (E) calcaneal eversion distance [CED] measurement.

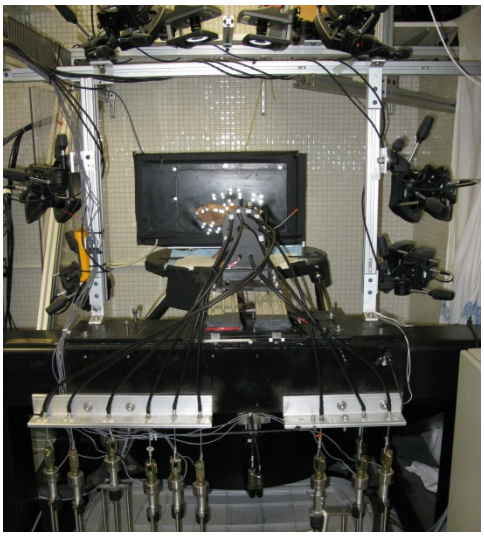

Figure 3.2: Robotic gait simulator (RGS) with mounted cadaveric specimen, pressure and force plates, linear actuators and retro-reflective motion analysis cameras.

The peak plantar pressure under the foot was measured with a Novel emed-sf pressure platform attached to the surface of the force plate. An AP radiograph was used to apply a mask to the data that defined the heel, medial midfoot, lateral midfoot, first through fifth metatarsals, hallux, and lesser toes. Center of pressure (CoP) data were analyzed using a method similar to De Cock[43]. The longitudinal foot axis was defined as a line from the most posterior, medial point on the pressure trace to a point over the second metatarsal head (Figure 3). The displacement of the CoP in the ML direction was defined with respect to the x-axis, perpendicular to the longitudinal foot axis. For analysis, the ML displacement was compared at four points in stance: 25%, 50%, 75%, and 90%.

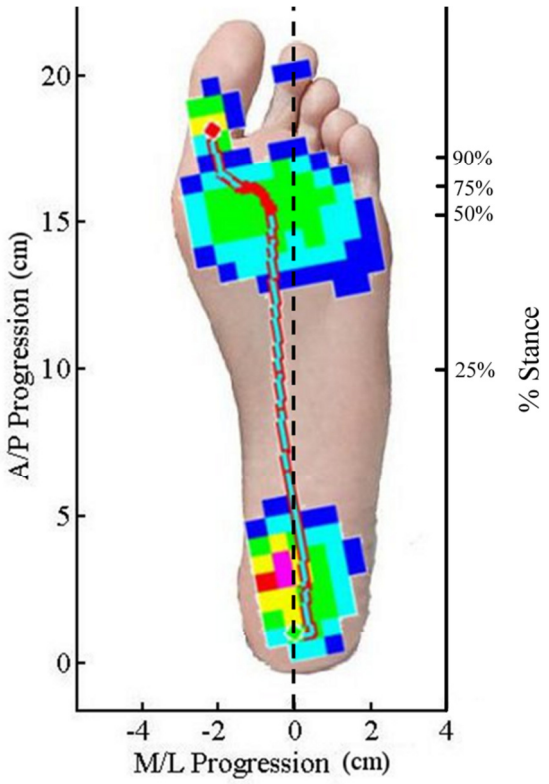

Figure 3.3: A representative center of pressure (CoP) progression for a flatfoot trial on the robotic gait simulator (RGS). Dotted lines indicate longitudinal foot axis.

The kinematics of individual foot bones were measured using an eight-camera Vicon system and a previously described ten-segment foot model[7]. Primary kinematic data included

range of motion (ROM) and average absolute difference between flatfoot and post-surgery (offset) during stance phase in all three cardinal planes for the talonavicular joint (Nav_Tal), the calcaneus with respect to tibia (Calc_Tib), and the first metatarsal with respect to talus (Met1_Tal).

After testing the flatfoot specimens on the RGS, LCL procedures were performed. One of each pair received the Evans (Figure4A) while the other received the Z-osteotomy (Figure 4B). All surgeries were performed by one of two orthopedic surgeons. For the Evans, the osteotomy was created at a right angle to the calcaneal neck approximately 10mm anterior to the calcaneal cuboid (CC) joint. The osteotomy was then opened to a length of 8-10mm, and a plastic wedge was inserted and fixed with a five hole, 25mm cervical vertebrae plate held in place with four 3.5mm diameter surgical screws (Synthes, West Chester, PA; Figure 4A). A distal vertical cut was made at approximately 10mm from the CC joint through the dorsal half of the calcaneal neck. A proximal vertical cut was made as posteriorly as possible without compromising the calcaneal tubericle. Last, a longitudinal cut was made joining the proximal and distal cuts to complete the Z. The osteotomy was opened 8-10mm and secured with surgical screws both superiorly and inferiorly across the longitudinal cut, and posteriorly through the calcaneus (Figure 4B). The procedure utilized more surgical screws than are normally seen clinically to bolster the surgery due to lack of healing with the cadavers. Additionally, plastic wedges were placed in the resulting openings from the dorsal and plantar cuts. After surgical correction, the feet were once again X-rayed and tested on the RGS. Simulation an FDL to TP surgical procedure, FDL was unloaded, while TP was load with 1.8 FDL forces to simulate hypertrophy[44,45].

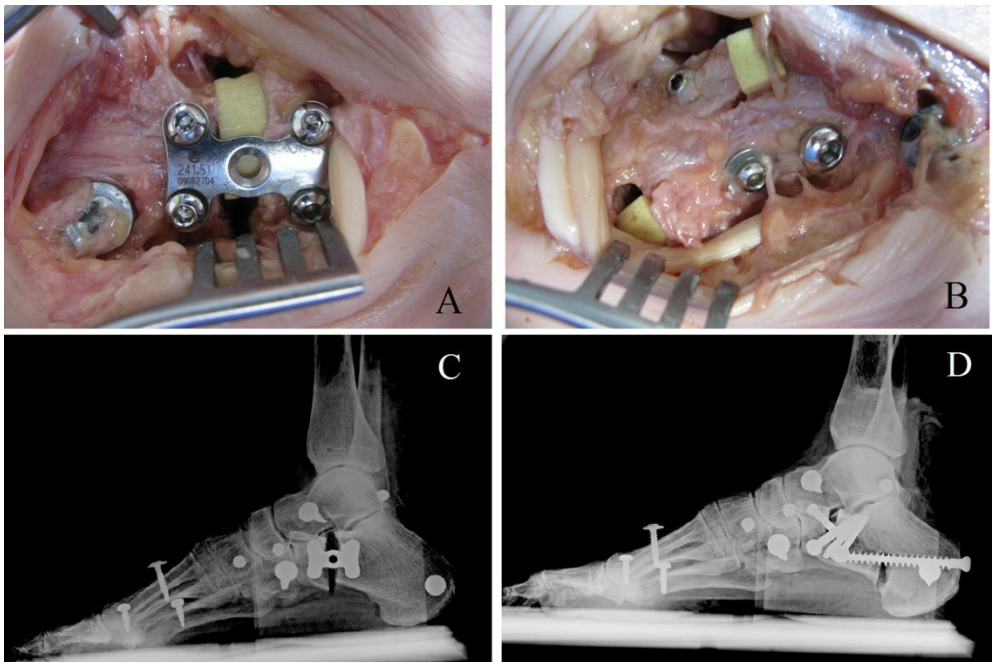

Figure 3.4: A specimen having received the (A) Evans lateral column lengthening and the (B) Z-osteotomy. The post-surgery M/L radiograph (C, D) is shown below each of the photographs. More screws than typically seen clinically were used to secure the surgical site and plastic wedges were used to maintain bony position. Note that hardware not associated with the fracture site was used to secure the kinematic markers.

For statistical analysis of the radiographic data, linear mixed effects regression of each X-ray measure was carried out to make pairwise comparisons of flatfoot vs. initial, post-surgical vs. initial and post-surgical vs. flatfoot. Linear mixed effects models were used to determine if there was a significant change in kinetic (peak pressure and CoP) and/or kinematic (ROM and offset) parameters from flatfoot to post-surgical trials, and if any of the changes differed by surgery. CoP models were adjusted for foot width, with model estimated means presented with foot width equal to the mean foot width for the study population (8.6cm). All analyses were carried out using R 2.14.0[46] and the lme4[47] package.

Results

After undergoing the flattening procedure, all X-ray parameters showed significant changes towards flatfoot (Table 1). The CPA decreased by 2.7° ($p=0.015$), the LTMA increased

by 7.7° ($p<0.0001$), and the NH decreased by 4.4mm ($p=0.0010$), all signifying a drop in the medial arch of the foot. The TNCA increased by 7.2° ($p<0.0001$), indicating forefoot abduction, and the CED increased by 6.2mm ($p=0.0005$), indicating hindfoot valgus. After receiving an LCL, all X-ray parameters showed significant arch restoration. Compared to flatfoot, the CPA increased by 3.6° ($p=0.0014$), the LTMA decreased by 6.0° ($p<0.0001$), and the NH increased by 4.7mm ($p=0.0006$), all signifying medial arch restoration. The TNCA decreased by 9.2° ($p<0.0001$), indicating forefoot adduction, and the CED decreased by 6.9mm ($p<0.0001$), indicating a less everted calcaneus. For all X-ray measures, there were no statistical differences when comparing initial to post-surgical foot shape, indicating that the original foot shape was restored. No differences were seen between feet where the spring ligament had been attenuated versus sectioned (data not shown).

Table 3.1: Mean and standard errors [SE] for initial X-ray measures and differences in initial vs. flatfoot, flatfoot vs. post-surgery, and initial vs. post-surgery ($p < 0.05$).

	Mean [SE] at initial	Mean [SE] change from: Initial→flat / flat→post-surg. / initial→post-surg.	p-value
Calcaneal pitch angle (°)	24.9 [2.4]	-2.7 [1.1] / +3.6 [1.1] / +1.0 [1.1]	0.015 / 0.0014 / 0.37
Lateral talometatarsal angle (°)	-2.6 [2.7]	+7.7 [1.0] / -6.0 [1.0] / +1.7 [1.0]	<0.0001 / <0.0001 / 0.094
Navicular height (mm)	33.9 [2.2]	-4.4 [1.3] / +4.7 [1.3] / +0.3 [1.3]	0.0010 / 0.0006 / 0.84
Talonavicular coverage angle (°)	22.3 [2.1]	+7.2 [1.3] / -9.2 [1.3] / -1.9 [1.3]	<0.0001 / <0.0001 / 0.14
Calcaneal eversion distance (mm)	5.8 [2.2]	+6.2 [1.6] / -6.9 [1.3] / +0.7 [1.6][c]	0.0005 / <0.0001 / 0.64

When comparing flatfoot to post-surgery X-ray measures between surgeries, there were no significant differences between the Evans and the Z-osteotomy (Table 2). Of note is that the LTMA had the greatest difference between paired feet at flatfoot (i.e., average flatfoot LTMA of feet receiving Evans versus Z was 3.6° and 6.6°, respectively); however, there were no differences in the correction provided by surgery types for the number of specimens tested.

Table 3.2: Mean and standard error [SE] values for measured X-rays at flatfoot and changes from flatfoot to post-surgery by surgery type ($p < 0.05$).

	Mean [SE] at flatfoot	Mean [SE] change from flatfoot to post-surgery	p-value
Calcaneal pitch angle (°)			
Evans	21.5 [2.6]	+2.5 [1.4]	0.27
Z	22.9 [2.6]	+4.7 [1.4]	
Lateral talometatarsal angle (°)			
Evans	3.6 [2.9]	-4.6 [1.3]	0.13
Z	6.6 [2.9]	-7.4 [1.3]	
Navicular height (mm)			
Evans	29.3 [2.4]	+4.2 [1.2]	0.53
Z	29.6 [2.4]	+5.2 [1.2]	
Talonavicular coverage angle (°)			
Evans	29.3 [2.2]	-8.0 [1.5]	0.25
Z	29.7 [2.2]	-10.3 [1.5]	
Calcaneal eversion distance (mm)			
Evans	11.6 [2.4]	-7.1 [1.5]	0.79
Z	12.4 [2.4]	-6.6 [1.5]	

Peak plantar pressures resulting from *in vitro* simulations at 25% BW on the RGS showed similar trends when compared to 100% BW *in vivo* walking trials (Figure 5)[48]. (Midfoot pressures at 25% BW were negligible and not report here.) Starting from the second metatarsal, peak pressure continuously dropped across the lateral forefoot regions (third to fifth metatarsal) in both *in vivo* and *in vitro* studies. In five of the seven regions, the 25% BW *in vitro* peak pressure was approximately a scaled representative of the full BW *in vivo* pressure data.

However, greater overall pressure was seen under the first ray (first metatarsal and hallux) in the RGS trials compared to *in vivo* data.

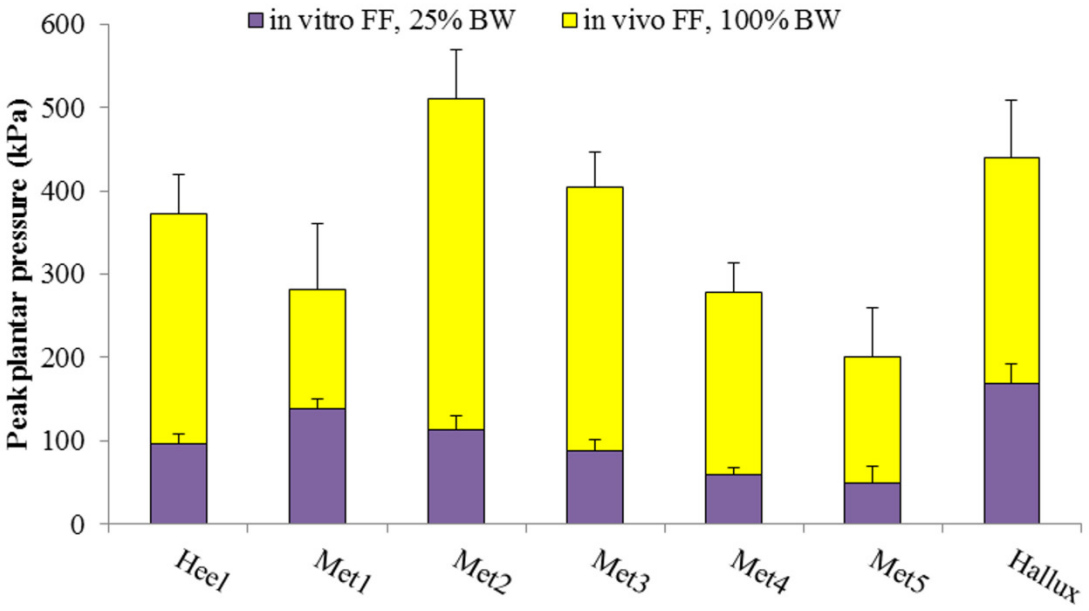

Figure 3.5: Average *in vitro* flatfoot (FF) pressure data (25% body weight [BW]) from current study for seven plantar regions (heel, first through fifth metatarsals [Met1-Met5], and hallux) compared to average *in vivo* FF pressure data (100% BW) for the same regions[48]. Note lesser toe data were not available from the literature.

The only significant difference in plantar pressure between the flatfoot and osteotomy procedures was an increase in peak pressure under the lateral forefoot regions (Table 3). Pressure under third, fourth and fifth metatarsals increased by 27kPa, 81kPa, and 77kPa respectively ($p = 0.017, 0.013, 0.007$) after receiving an LCL procedure. There was no difference elsewhere post-surgery, nor between surgeries (Table 3). There were also no significant differences between trials where FDL was active or inactive (data not shown), but there small decreases in heel and lesser toe pressure when TP was inactive (data not shown). However, since our primary area of interest was the load bearing regions of the forefoot (hallux and metatarsals), these differences were not considered critical.

Table 3.3: Mean and standard error [SE] pressure at flatfoot and change in pressure from flatfoot to post-surgery for all feet, and separated by surgery type ($p < 0.05$).

Plantar Region	Surgery Type	Mean pressure at flatfoot (kPa)	Mean change from flatfoot to post-surgery (kPa)	p-value (flatfoot to post-surgery / Evans vs. Z)
First Metatarsal	Combined	138 [13]	-23 [27]	0.39 / 0.70
	Z	121 [20]	-29 [24]	
	Evans	155 [15]	-17 [51]	
Second Metatarsal	Combined	114 [16]	-1 [15]	0.94 / 0.50
	Z	119 [29]	-12 [28]	
	Evans	109 [17]	+10 [14]	
Third Metatarsal	Combined	88 [13]	+27 [11]	0.017 / 0.27
	Z	96 [14]	+15 [15]	
	Evans	80 [15]	+40 [15]	
Fourth Metatarsal	Combined	59 [9]	+81 [30]	0.013 / 0.13
	Z	64 [9]	+63 [44]	
	Evans	54 [17]	+100 [44]	
Fifth Metatarsal	Combined	50 [20]	+77 [26]	0.007 / 0.17
	Z	46 [15]	+45 [19]	
	Evans	53 [32]	+109 [47]	
Hallux	Combined	168 [25]	-33 [27]	0.21 / 0.59
	Z	165 [42]	-48 [32]	
	Evans	170 [29]	-19 [45]	
Lesser Toes	Combined	78 [7]	-16 [11]	0.14/0.95
	Z	63 [8]	-15 [15]	
	Evans	92 [10]	-17 [17]	
Heel	Combined	97 [12]	-5 [9]	0.54 / 0.39
	Z	97 [15]	+1 [13]	
	Evans	96 [11]	-12 [12]	

At all four selected points of stance, the CoP was medial of the longitudinal axis for the flatfoot simulations. Post-surgery, all four points of stance showed a significant lateral shift in CoP position, ranging from 0.59cm at 25% stance to 1.05 cm at 75% stance (Table 4). When comparing the surgical techniques, there were no differences between the Evans and the Z-osteotomy at any of the selected points in stance (Table 5).

Table 3.4: Mean [SE] CoP location at flatfoot and change in CoP location from flatfoot to post-surgery ($p<0.05$).

% Stance	Mean [SE] at flatfoot (cm)	Mean change [SE] from flatfoot to post-surgery (cm)*	p-value
25%	-0.55 [0.16]	+0.59 [0.22]	0.013
50%	-0.83 [0.20]	+0.93 [0.30]	0.0051
75%	-1.38 [0.19]	+1.05 [0.30]	0.0023
90%	-2.02 [0.16]	+0.77 [0.31]	0.020

* (+) represents a lateral shift from the flatfoot mean.

Table 3.5: Mean [SE] CoP location separated by surgery.

% Stance	Mean [SE] for Evans (cm)	Mean [SE] for Z (cm)	p-value
25%	-0.09 [0.12]	0.19 [0.32]	0.38
50%	-0.04 [0.18]	0.25 [0.44]	0.41
75%	-0.50 [0.23]	-0.14 [0.41]	0.30
90%	-1.49 [0.44]	-1.01 [0.40]	0.23

Kinematic data yielded two significant differences from flatfoot to post-surgery (Table 6): there was a significant increase in transverse plane ROM for Calc_Tib post-surgery (0.7°, $p = 0.046$) and a decrease in sagittal plane ROM for Met1_Tal (2.8°, $p = 0.017$). When comparing the Evans to the Z-osteotomy, the only significant difference was a greater decrease in sagittal plane Met1_Tal ROM for the Z (-4.8°) than the Evans (-0.7°). Offset data showed a post-surgical -9.4° shift (adduction) in transverse plane for Nav_Tal ($p = 0.0073$) (Table 7), indicating more talonavicular coverage. Additionally, significant eversion in the Met1_Tal was seen in the frontal plane ($p = 0.013$).

Table 3.6: Mean [SE] values for range of motion (ROM) at flatfoot and difference between flatfoot and post-surgery ($p < 0.05$).

Child bone with respect to parent bone ROM (°)	Plane	Surgery	Flatfoot mean [SE]	Mean change from flatfoot to post-surgery [SE]	p-value (flatfoot to post-surgery / Evans vs. Z)
Calcaneus_Tibia	Frontal	Combined	8.3 [0.8]	+0.6 [0.8]	0.43 / 0.36
		Evans	9.2 [1.3]	+0.2 [1.1]	
		Z	7.5 [0.8]	+1.1 [1.2]	
	Transverse	Combined	6.7 [0.5]	+0.7 [0.4]	0.046 / 0.073
		Evans	6.2 [0.6]	+1.3 [0.3]	
		Z	7.2 [0.8]	+0.2 [0.6]	
	Sagittal	Combined	19.9 [0.7]	-0.7 [1.0]	0.48 / 0.14
		Evans	20.9 [1.0]	-1.3 [1.7]	
		Z	18.8 [0.9]	-0.0 [1.1]	
Navicular_Talus	Frontal	Combined	15.2 [0.9]	-0.6 [1.2]	0.61 / 0.88
		LCL	16.0 [1.5]	-0.5 [1.8]	
		Z	14.4 [0.9]	-0.8 [1.8]	
	Transverse	Combined	10.6 [0.8]	+0.3 [1.2]	0.77 / 0.052
		Evans	9.4 [0.6]	+2.3 [1.3]	
		Z	11.8 [1.4]	-1.6 [1.8]	
	Sagittal	Combined	6.4 [0.8]	-0.3 [1.1]	0.76 / 0.21
		Evans	5.8 [0.9]	+0.8 [1.7]	
		Z	6.9 [1.4]	-1.5 [1.4]	
First Metatarsal_ Talus	Frontal	Combined	11.0 [0.9]	+0.4 [0.9]	0.68 / 0.96
		Evans	11.7 [1.6]	+0.3 [1.0]	
		Z	10.4 [0.8]	+0.4 [1.6]	
	Transverse	Combined	13.0 [0.9]	+1.0 [1.4]	0.450 / .057
		Evans	12.2 [1.1]	+2.9 [2.1]	
		Z	13.8 [1.5]	-0.9 [1.7]	
	Sagittal	Combined	14.6 [0.9]	-2.8 [1.1]	0.017 / 0.019
		Evans	13.4 [1.4]	-0.7 [1.2]	
		Z	15.8 [0.9]	-4.8 [1.5]	

Table 3.7: Mean and standard [SE] kinematic shift (offset) for the entire stance phase from flatfoot to post-surgery. + = inversion (frontal), abduction (transverse), plantar flexion (sagittal) ($p < 0.05$).

Child with respect to parent bony offset angle (°)	Plane	Mean [SE]	p-value
Calcaneus_Tibia	Frontal	-3.1 [2.6]	0.23
	Transverse	2.9 [3.9]	0.44
	Sagittal	1.7 [3.0]	0.57
Navicular_Talus	Frontal	-5.7 [3.6]	0.12
	Transverse	-9.4 [3.2]	0.0073
	Sagittal	5.2 [6.2]	0.39
First Metatarsal_ Talus	Frontal	-10.5 [3.9]	0.013
	Transverse	0.1 [3.0]	0.98
	Sagittal	-4.0 [2.4]	0.10

Discussion

This study was motivated by the prevalence of flatfoot and the lack of objective investigation into the Z-osteotomy. The goals of this study were to develop a physiologically realistic cadaveric flatfoot model using evidence-based ligament attenuation, then compare and contrast the well-established Evans osteotomy with the Z-osteotomy.

Though not indicative of severe Stage II, there was evidence that a flatfoot was created using the proposed model. Analysis of the radiographic measurements showed significant changes in all five of the measures of interest. Ellis et al. subdivided Stage II flatfoot (IIa: less severe, IIb: more severe) and found an LTMA between 4.2° (IIa) and 21.8° (IIb), signifying a more dorsiflexed first metatarsal[49]. Using the same categorization, the mean flatfoot LTMA (5.1°) in the current study would classify as flat, though not severe. Ellis et al. also showed a TNCA between 13.6° (IIa) and 42.8° (IIb), signifying more abduction in the forefoot. A mean flatfoot TNCA of 29.5° in our study showed an excellent model of flatfoot in the transverse plane. A study by Arangio et al. reported a CED for patients with adult acquired flatfoot between 12 and 23mm[30]. The increase in CED for our study from 5.8mm to 12.0mm falls into the range of less severe flatfoot. The NH decrease of 4.4mm intuitively shows a drop in the medial arch of the foot, and the CPA (flatfoot mean of 22.2°) was the only metric that did not fall within a range consistent with flatfoot, as Sangeorzan et al.[19] reported an average preoperative flatfoot CPA of 3.2°.

Though not to the level reported in clinical *in vivo* studies, modest correction in all X-ray parameters was seen after the LCL procedures were performed. This could be attributed to the fact that the *in vitro* creation of flatfoot was not as severe as those seen clinically. Radiographical

analysis showed significant improvement in foot shape post-surgery, with no differences resulting between surgery type. *In vivo* studies have shown improvement of the LTMA with an increase in first metatarsal plantar flexion that ranged from 8.7° to 13.0°[19,49] after receiving the Evans procedure. Our study showed a more modest change of 6.0°. Improvement in TNCA was reported between 2.4° and 26.0°[19,49] post-operative with the navicular covering more of the talar head. Our study showed a mean correction of 9.2°. Saltzman and El-Khouri[15] reported a population average of -1.6mm (slight inversion); however, our post-surgical result (6.9mm) lies just outside one standard deviation. The post-surgical NH of 34.2mm is close to results from Williams et al. using a very similar measure, who reported an NH ranging from 39.7 to 34.6mm for a normal population at 10 to 90% weight bearing, respectively[40]. Finally, though improvement was seen in the CPA, very little was needed due to the original lack of sagittal plane collapse of the calcaneus.

This study showed a shift of peak plantar pressures and CoP laterally for both surgeries. The Evans and Z-osteotomy did not significantly differ, indicating that similar plantar pressure distributions will be seen when comparing the surgical outcomes. While analysis showed a shift of pressure to the more lateral region of the forefoot after surgery, no corresponding decrease in pressure under the medial forefoot was noted; however unlike a clinical event, no attempt was made to increase plantar flexion of the medial column by Cotton osteotomy or midfoot fusion. Tien et al. simulated midstance using intact cadavers and reported a mean peak pressure increase of 20kPa in fifth metatarsal pressure in feet receiving the Evans procedure[50]. A similar study showed that lateral forefoot pressure increased from 24.6 to 33.9kPa after the Evans procedure with simulated FDL transfer[51]. As with our study, previous work using cadaveric specimens positioned at midstance have shown that no significant change occurs in the medial region of the

forefoot when using scaled BW[5,51]. An *in vivo* study by Ellis et al. reported mean fifth metatarsal pressures of 63kPa for patients who reported no pain following the Evans procedure and up to 77kPa for patients who reported pain[4].

Kinematic flatfoot and post-surgical results agreed with the literature. Comparing mean flatfoot ROM from this study with a previous study using neutrally aligned feet and the RGS[7], the current study had decreased mean ROM in all three planes (coronal, transverse, sagittal) for Calc_Tib, Nav_Tal, and Met1_Tal. An *in vivo* multi-segment foot model study by Ness et al.[52] also found that in general subjects with PTTD has less ROM throughout the foot. Post-surgically, we found adduction of the Nav_Tal offset, agreeing with our X-ray data and indicating realignment of the foot in the transverse plane. Additionally, the decrease of 2.8° post-surgery in the sagittal ROM of the Met1_Tal could be the result of soft tissue tightness after the osteotomies. Marks et al. found decreased ROM post-surgically in both the forefoot and hindfoot. Finally, the difference in ROM of the Met1_Tal complex was the only difference seen between surgeries, meaning this relationship may be most sensitive to the type of surgical correction.

This study had several limitations. First, due to methodological changes, we simulated a Stage II flatfoot with TP active for the first 6 feet, but it was inactive for the rest. Statistical analysis showed a few peak pressure differences, but none in the forefoot. Further, the effect of TP was not the focus of this study, therefore these differences were not critical. Next, soft tissue procedures (e.g., spring ligament repair) are often performed coincident to an LCL; however, our study emphasized the calcaneal osteotomies with an FDL transfer, but no other soft tissue procedures were performed. Regarding target kinematic and kinetic data used as inputs into the RGS, we generated the post-surgery cadaveric simulations with the same pre-surgery kinematic

inputs. Most likely patients will walk differently post-surgically; however, different gait patterns could further confound the analysis. Additionally, the RGS GRFs were scaled to 25% BW, with simulations that were performed on average six times slower than *in vivo* stance phase, possibly affecting kinematic and kinetic data. Finally, although the change in the mean radiographic measures indicated flatfoot to some level (except for CPA), only mild flatfoot was attained in specimens when compared to clinical studies. Pes planus often develops over many years while the current model attempted to induce flatfoot over a matter of hours.

This study presents both static and dynamic evidence that our cadaveric flatfoot model is, in general, a good representation of pes planus. Additionally, the Evans and Z-osteotomy LCL procedures are similar in their ability to correct flatfoot. Based on the similar biomechanical function and the potential for improved bone contact area (and subsequent healing), the Z-osteotomy should be considered a viable alternative to the Evans.

Chapter 4: Conclusion

The integrity of the foot and ankle is very important when it comes to health and quality of life. Foot and ankle biomechanics are complex, and in many cases, the mechanisms of therapeutic and/or restorative medical procedures are not completely understood. Further research in this field is vital to advancing the current knowledge of such an important and intricate structure. Robotic gait simulation (RGS) provides an avenue for researchers to invasively and dynamically study foot and ankle structure and morphology. Furthermore, this technology allows for the investigation of biomechanical changes resulting from surgical treatments to be studied more rigorously using invasive techniques (e.g., bone pins) that would not be possible with living subjects. However, methods must be developed that can mimic medical procedures (e.g., load-bearing radiographs or surgical outcomes) in a laboratory setting using cadaveric specimens. Physiologic accuracy must also be taken into account to some degree in order to utilize gait simulation to its fullest potential. The work accomplished in this thesis has looked to address these challenges by:

1. *Developing a repeatable method to collect and measure clinically relevant radiographs using cadaveric specimens.*

In order to accurately diagnose and/or quantify abnormalities in cadaver specimens, researchers must be able to reproduce clinical X-ray procedures which often require the foot to be in a load bearing position. This work utilized a custom designed loading frame that applied and held a 25% body weight load to a specimen throughout the duration of radiograph collection. Three common views were collected in order to assess foot shape: the medial/lateral, anterior/posterior, and hindfoot alignment views. From these three views, five clinical

measurements were used to quantify foot shape: calcaneal pitch angle, lateral talometatarsal angle, navicular height, talonavicular coverage angle, and calcaneal eversion distance. This study demonstrated that our loading technique and measurement methods are highly repeatable for collecting clinically relevant foot and ankle radiographs using cadaveric specimens. Future work into accuracy of the measurements would provide an even more robust validation of the method used to analyze cadaveric radiographs.

2. *Developing a more realistic cadaveric flatfoot model for use in dynamic gait simulations where pes planus is to be investigated.*

Previous studies performed within our lab group developed a flatfoot model through the attenuation of selected ligaments shown to be involved in flatfoot followed by cyclic axial loading. This past work relied upon external visual confirmation that a flatfoot was achieved, but did not attempt to validate the model using clinical measures. This thesis added to past work by including radiographic analysis (as described in objective #1 above) as part of the process to ensure flatfoot was being achieved. Additionally, biomechanical evidence of flatfoot was also investigated (e.g., plantar pressure and bony kinematics). Radiographic data confirmed a mild representation of Stage II (e.g., flexible) flatfoot. Additionally, there was radiographic evidence that complete sectioning of the spring ligament does not yield a more severe flatfoot than attenuation of the spring ligament. Results from dynamic gait simulation, including kinetics and kinematics, were consistent with pes planus, including more medially distributed plantar pressures and decreases in overall bony ranges of motion. The primary limitation of the model included a calcaneal pitch angle that did not fall into the common flatfoot range. Future improvements to the model could include statically or dynamically loading the Achilles tendon during cycling to induce greater levels of arch collapse by increasing the load on the forefoot.

3. *Advancing biomechanical research of surgical procedures that correct severe Stage II symptomatic flatfoot.*

Using the above methods to induce and quantify flatfoot in cadaveric specimens, this thesis ventured further into flatfoot research by statically and dynamically comparing and contrasting the results of two flatfoot corrective procedures. Stage II flatfoot is often treated with lateral column lengthening (LCL) procedures such as the Evans LCL, and more recently the Z-osteotomy. The Z-osteotomy has more bone-on-bone contact for improved healing, and is thought to minimize increases in lateral pressure as compared to the Evans. This study found that the Z-osteotomy and Evans LCL are similar in their ability to address the flatfoot deformity. Peak plantar pressures were higher in feet that had an LCL procedure, but there were no significant differences between the Evans and the Z-osteotomy. Additionally, very few kinematic differences were observed when comparing the results from the two procedures. Based on the similar biomechanical function and the potential for improved healing due to increased bone contact area, the Z-osteotomy should be considered a viable, if not preferred, alternative to the Evans LCL.

4. *Investigation into how foot type (e.g., pes planus, pes cavus) affects tibial kinematics.*

Cadaveric gait simulators employ six degree-of-freedom tibial kinematic and ground reaction force (GRF) curves as target inputs. For example, the aforementioned study investigating the Evans and Z-osteotomy (objective #3) used data from symptomatic pes planus subjects to generate tibial kinematic and GRF curves to drive the RGS. This study, as part of a collaborative effort (first author: Eric Whittaker), aimed to examine the differences in tibial kinematics and GRF between the following common foot types: pes cavus (PC), neutrally aligned (NA), asymptomatic pes planus (APP), and symptomatic pes planus (SPP). Significant

differences were observed between PC and NA, most notably in sagittal and transverse plane rotations, and there were small, non-significant differences between SPP or APP and NA. Future studies on the RGS should take into account changes in tibial kinematic and GRF curves, as differences in these parameters may play a key role in biomechanical response of the foot during gait. Future work could include the development a database containing tibial kinematic and GRF curves for subjects with a variety of foot shapes, including foot shapes resulting from surgical corrective procedures (e.g., after receiving an LCL procedure).

To summarize, the main goal of my research was to improve the fidelity in which flatfoot and corresponding corrective techniques are implemented and studied using robotic gait simulation. From this work, future studies addressing foot shape will have an example of how to quantify bony radiographic measurements, induce flatfoot, and analyze data from RGS trials. These biomechanical analyses will allow clinicians to make more informed decisions about surgical procedures used to correct flatfoot. Small advancements and other potential avenues of research into mechanisms that could improve the biofidelity of the RGS were also investigated and noted. Future efforts should be made to continuously improve the RGS while also answering clinical questions using cadaver models, which provide information that would otherwise be difficult or impossible to collect *in vivo*.

Appendix A: The Effect of Foot Type on Tibial Kinematics

Abstract

The six degree-of-freedom kinematics of the tibia hold important information for clinical gait assessment and lower extremity biomechanics research, especially cadaveric gait simulation. This study aimed to examine the differences in tibial kinematics and ground reaction forces (GRF) between the following common foot types: pes cavus (PC), neutrally aligned (NA), asymptomatic pes planus (APP), and symptomatic pes planus (SPP). There were significant differences between PC and NA, most notably in sagittal and transverse plane rotations, and there were small but not clinically meaningful differences between SPP or APP and NA. Clinical assessment of lower extremity biomechanics should consider the effect of foot type on tibial motion, as there may be implications for clinical applications like the use of foot orthoses to treat knee osteoarthritis. Moreover, cadaveric gait simulators should employ different six degree-of-freedom tibial kinematic and GRF curves for the common foot types.

Introduction

Common foot types include flat arched (pes planus), neutrally aligned, and high arched (pes cavus)[53]. While there is some debate in the literature, it is thought that varying bony alignments of these foot types can lead to biomechanical changes in the proximal segments and joints. For example, tibial internal rotation coupled with hindfoot eversion has been associated with foot type and possible injury risk[54]. Additionally, lateral wedge foot orthoses, which can align foot bones similarly to that seen in pes planus (e.g., rearfoot eversion), have been used to treat medial knee osteoarthritis[55]. Exploring the six degree-of-freedom (DOF) motion of the tibia

as related to foot type will provide a more complete picture of the kinematics and their potential contribution to lower extremity injuries. Additionally, cadaveric gait simulation has become a valuable part of foot and ankle research, allowing for invasive exploration of the foot that could not be easily accomplished *in vivo*[56,57]. To accurately simulate gait using cadaver feet, the motion of the tibia with respect to the ground is often employed; thus, it is important to know if tibial kinematics differ significantly between foot type.

The purpose of this study was to identify the effects of foot type on tibial kinematics for use in both *in vivo* and *in vitro* biomechanics applications. A complete description of the tibial kinematics will provide a better understanding of the effects of abnormal foot types on proximal segments, and supply valuable information to groups performing *in vitro* gait simulation.

Methods

Ten subjects from each of the following foot types were included in this study, for a total of 40 subjects: pes cavus (PC), neutrally aligned (NA), asymptomatic pes planus (APP), and symptomatic pes planus (SPP). Foot type was pre-screened by an orthopedic surgeon using a clinical exam and X-rays.

An eight-camera Vicon system (Vicon Motion Systems Inc**,** Oxford, UK) collecting at 120 Hz was used to capture five overground walking trials per subject. Six-DOF tibial kinematics were determined from markers on the medial and lateral malleoli and femoral epicondyles. The origin of the tibia coordinate system was the ankle joint center, and the origin of the lab coordinate system was a point directly under the medial malleolus at the instant of heel strike. The six kinematic parameters examined in this study are as follows: anterior/posterior (AP), superior/inferior (SI), and medial/lateral (ML) displacement; and frontal plane, transverse

plane, and sagittal plane rotation. Ground reaction force (GRF) data was collected with two Bertec force plates (Bertec Corp, Columbus, OH). Additionally, overall range of motion (ROM) of the kinematic data and range of the force data were calculated.

Linear mixed effects regression was used to determined differences between NA and APP, SPP or PC. Kinematic and kinetic time-series data were assessed at each of 200 normalized data points, with the Benjamimi-Hochberg correction used to determine significance ($p<0.05$). ROM and range data significance was set at $p<.0083$ using Bonferroni's correction for multiple comparisons (.05/6). Analyses were carried out using R 2.14.1[58] and the lme4 package[47].

Results

Of the 40 subjects tested, one PC subject and one SPP subject were excluded due to missing force plate data. Most significant differences in tibial motion occurred between PC and NA for sagittal rotation, transverse rotation, and SI displacement (Table A.1, Figure A.1). Sagittal rotation had significant differences between PC and NA during the last 30% of stance phase. Median tibia transverse plane rotation for PC was 8.7° more externally rotated than NA subjects throughout the majority of stance. Median ankle joint center was 8.4 mm more superior for PC compared to NA (SI displacement) from approximately 10-50% stance. There were also differences for ML displacement between APP or SPP and NA during the first 50% of stance, with the ankle joint center of APP or SPP being more medial. There were very few differences in the GRF data between foot types. For kinematic range of motion (ROM), SPP showed 3.2˚ less ROM than NA in the sagittal plane (Table A.2). There were no other significant findings for kinematic ROM or force range.

Table A.1: Median differences and range of differences in kinematics and ground reaction forces between NA and the other foot types. Significant tests indicate the number of differences among 200 data points during stance phase. Figure A.1 shows temporal distribution of differences.

	Median differences [range] from NA			significant
Kinematic Variable	PC-NA	APP-NA	SPP-NA	tests
Sagittal rot. (°)	1.7 [-1.0, 7.1]	2.2 [0.9, 3.8]	1.9 [-0.2, 5.0]	58[a]
Frontal rot. (°)	2.4 [-1.7, 2.8]	-0.4 [-5.3, 0.9]	-0.1 [-2.2, 0.2]	0
Transverse rot. (°)	8.7 [6.1, 11.2]	-0.9 [-3.1, -0.2]	2.4 [1.8, 2.9]	194[a]
ML disp. (mm)	-1.8 [-3.3, 9.0]	2.6 [-0.8, 4.2]	3.4 [0.2, 14]	98[b]
AP disp. (mm)	-7.3 [-38, -5.2]	4.0 [-22, 5]	2.2 [-22, 3.1]	0
SI disp. (mm)	8.4 [-7.1, 10.2]	-1.9 [-7.2, 1.6]	1.0 [-6.7, 4.8]	87[a]
ML GRF (N/BW)	0.002 [-0.019, 0.011]	0.0076 [-0.002, .019]	0.006 [-0.008, 0.015]	3
AP GRF (N/BW)	-0.001 [-0.047, 0.022]	0.000 [-0.041, 0.022]	0.000 [-0.058, 0.026]	0
SI GRF (N/BW)	-0.03 [-0.10, 0.06]	-0.01 [-0.11, 0.03]	-0.03 [-0.13, 0.04]	2

[a] main differences between pes cavus (PC) and neutrally aligned (NA)
[b] main differences between asymptomatic pes planus (APP) or symptomatic pes planus (SPP) and NA
GRF = ground reaction force; ML = medial/lateral; AP = anterior/posterior; SI = superior/inferior; disp. = displacement; rot. = rotation

Table A.2: Mean ROM (displacement and rotation) or range (GRF) for NA and between NA and other foot types.

	Mean [SE]	Mean range or range of motion [SE] from NA			
Kinematic Variable	NA	PC-NA	APP-NA	SPP-NA	p-value
Sagittal rot. (°)	59.1 [1.7]	-6.7 [2.4]	1.0 [2.4]	-3.2 [2.4]	0.01[a]
Frontal rot. (°)	26.6 [2.3]	2.3 [3.4]	-5.9 [3.3]	-2.1 [3.4]	0.11
Transverse rot. (°)	10.0 [1.0]	-0.4 [1.4]	-1.6 [1.4]	0.9 [1.4]	0.36
ML disp. (mm)	22.0 [2.4]	-3.7 [3.5]	-0.9 [3.4]	-1.7 [3.5]	0.77
AP disp. (mm)	187.2 [8.7]	-30.5 [12.6]	-21.7 [12.3]	-16.7 [12.6]	0.12
SI disp. (mm)	103.5 [3.7]	-14.2 [5.4]	-3.3 [5.3]	1.0 [5.4]	0.04
ML GRF (N/BW)	0.106 [0.007]	0.018 [0.01]	0.001 [0.01]	-0.007 [0.01]	0.13
AP GRF (N/BW)	0.368 [0.019]	-0.052 [0.027]	-0.055 [0.026]	-0.074 [0.027]	0.58
SI GRF (N/BW)	1.117 [0.02]	-0.018 [0.029]	-0.032 [0.028]	-0.049 [0.029]	0.39

[a] Significant pairwise difference between neutrally aligned (NA) and symptomatic pes planus (SPP) ($p<0.0083$)
PC = pes cavus; APP = asymptomatic pes planus; GRF = ground reaction force; ML = medial/lateral; AP = anterior/posterior; SI = superior/inferior; SE = standard error; disp. = displacement; rot. = rotation

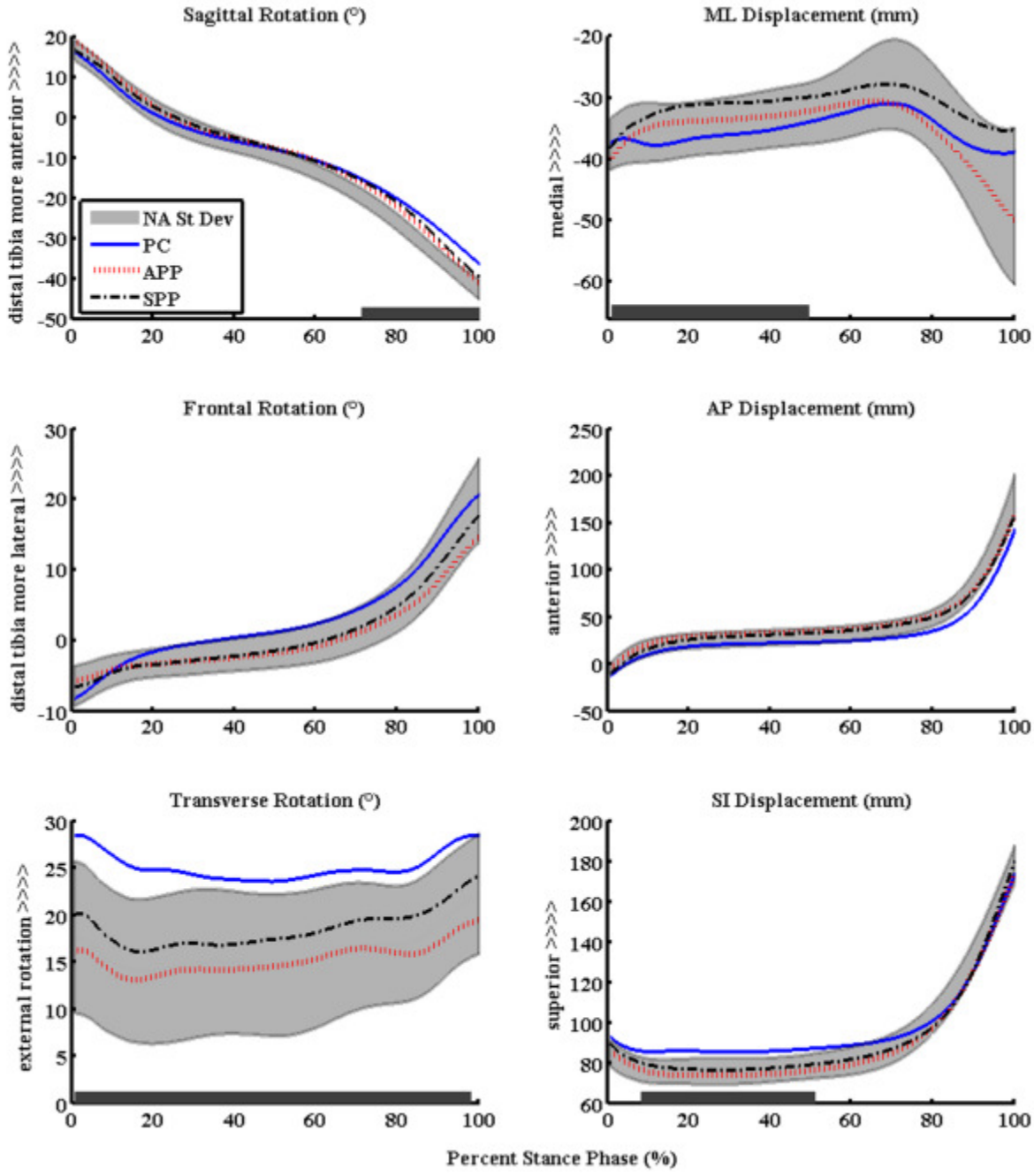

Figure A.1: Mean six degree-of-freedom tibial kinematics during stance phase. Rotations and displacements relative to ankle joint center. Dark grey bars along x-axis indicate regions of statistical difference from neutrally aligned (NA). Most differences between pes cavus (PC) and NA or asymptomatic pes planus (APP)/symptomatic pes planus (SPP) and NA (see Table A.1). ML = medial/lateral; AP = anterior/posterior; SI = superior/inferior.

Discussion

A thorough description of the six-DOF tibial kinematics during stance phase for the common foot types can provide both important clinical and research-related information. The development of gait simulators has allowed for invasive exploration of foot function, and often requires tibial motion as an input to drive simulated motion[11]. Since foot type has been shown to have some effects on lower extremity biomechanics[54,59], it is important to determine if gait simulation requires different tibial kinematic inputs for the different foot types. Additionally, identifying these differences may shed light on injury mechanisms, basic lower extremity biomechanics, or specific applications like the effects of foot orthoses to treat knee pain.

The differences found in tibial kinematic parameters support the descriptions of foot type in the literature. For example, PC subjects were shown in this study to have more externally rotated tibias than NA throughout stance phase; similarly, Nawoczenski et al. reported more external rotation for PC than pes planus (PP)[60]. The more superior ankle joint center in PC subjects from 10-50% stance can be attributed to the hindfoot varus and dorsiflexion seen in PC[61]. Tibial internal rotation excursion (transverse plane ROM) was not significant in this study, but Williams et al.[54] has shown the ratio of hindfoot eversion excursion to tibial internal rotation excursion to be associated with foot type. While this ratio was not examined directly in the current study, tibial transverse plane motion may be clinically important and should be included when performing gait simulations. Finally, Butler et al. reported that the addition of a lateral wedge orthosis led to decreased knee adduction moment and increased rearfoot eversion ROM, peak, and moment, although the relationship between the knee and ankle was not significant[55]. These results indirectly suggest the importance of assessing tibia kinematics as related to foot

type, as some relationship exists between knee biomechanics and the frontal plane position of the foot, which is an important component of foot type.

While flatfoot subjects (SPP and APP) showed a more medial ankle joint center position than NA during the first 50% of stance, these differences were small, averaging less than 3.4mm. The dorsiflexed medial forefoot[62] and adducted hindfoot[63] that often characterize pes planus would contribute to this medial shift; however, such small changes are not likely to have a clinically significant meaning.

Pain level may have had a significant effect on sagittal plane tibial motion. Compared to NA subjects, SPP subjects showed less ROM, and PC subjects showed less overall rotation during the last 30% of stance. SPP and PC subjects were candidates for ankle surgery, and had clinically significant pain levels; thus, kinematic differences may have been a learned response from pain guarding during the extremes of ankle plantar flexion and dorsiflexion.

GRFs showed very few differences in foot type. Nachbauer and Nigg reported no differences in peak GRFs between foot types[64], while Williams et al. showed PC to have greater vertical GRF loading rate[54]. While loading rate and timing was not quantified directly in this study, these parameters should be considered in clinical analysis and when performing gait simulation.

This study has several limitations. First, the absolute values of reported tibial motion are unique to the coordinate systems used for this study, and cannot be directly compared to other studies. Next, while the sample size was selected due to statistically significant results found in a previous study using the same sample size, more subjects per group may have resulted in more significant differences. Finally, this study explores a specific set of kinematic variables related to the tibia; however, there are many other kinematic and kinetic variables of the other leg segments

and joints (e.g., moments, powers, velocities) that may have additional differences between foot types.

Overall, this study shows that there are no clinically meaningful differences between the tibial kinematics of flatfeet and NA, but that differences exist between PC and NA, most notably in sagittal and transverse plane rotations. Clinical assessment of tibial motion as related to foot type should focus on these cardinal planes, while gait simulation should employ different six-DOF tibial kinematic and kinetic curves for the varying common foot types.

References

1. **Dunn, J. E.; Link, C. L.; Felson, D. T.; Crincoli, M. G.; Keysor, J. J.; and McKinlay, J. B.:** Prevalence of Foot and Ankle Conditions in a Multiethnic Community Sample of Older Adults. *American Journal of Epidemiology,* 159(5): 491-498, 2004.

2. **Myerson, M. S.:** Adult acquired flatfoot deformity: treatment of dysfunction of the posterior tibial tendon. *Instructional course lectures,* 46: 393-405, 1997.

3. **Arangio, G. A., and Salathe, E. P.:** A biomechanical analysis of posterior tibial tendon dysfunction, medial displacement calcaneal osteotomy and flexor digitorum longus transfer in adult acquired flat foot. *Clinical Biomechanics,* 24(4): 385-390, 2009.

4. **Ellis, S. J.; Yu, J. C.; Elliott, A.; O'Malley, M.; Deland, J.; and Johnson, A. H.:** Plantar pressures in patients with and without lateral foot pain after lateral column lengthening. *Journal of Bone and Joint Surgery,* 92(1): 81-91, 2010.

5. **Logel, K. J.; Parks, B. G.; and Schon, L. C.:** Calcaneocuboid distraction arthrodesis and first metatarsocuneiform arthrodesis for correction of acquired flatfoot deformity in a cadaver model. *Foot and Ankle International,* 28(4): 435-40, 2007.

6. **Griend, R. V.:** Lateral column lengthening using a "Z" osteotomy of the calcaneus. *Techniques in Foot and Ankle Surgery,* 7(4): 257-263, 2008.

7. **Whittaker, E. C.; Aubin, P. M.; and Ledoux, W. R.:** Foot bone kinematics as measured in a cadaveric robotic gait simulator. *Gait & Posture,* 33(4): 645-650, 2011.

8. **Lee, D. G., and Davis, B. L.:** Assessment of the effects of diabetes on midfoot joint pressures using a robotic gait simulator. *Foot and Ankle International,* 30(8): 767-772, 2009.

9. **Blackman, A. J.; Blevins, J. J.; Sangeorzan, B. J.; and Ledoux, W. R.:** Cadaveric flatfoot model: Ligament attenuation and Achilles tendon overpull. *Journal of Orthopaedic Research,* 27(12): 1547-1554, 2009.

10. **Jackson, L. T.; Aubin, P. M.; Cowley, M. S.; Sangeorzan, B. J.; and Ledoux, W. R.:** A robotic cadaveric flatfoot analysis of stance phase. *Journal of Biomechanical Engineering,* 133(5), 2011.

11. **Aubin, P. M.; Whittaker, E.; and Ledoux, W. R.:** A robotic cadaveric gait simulator with fuzzy logic vertical ground reaction force control. *IEEE Transactions on Robotics,* 28(1): 246-255, 2012.

12. **Deland, J. T.; de Asla, R. J.; Sung, I. H.; Ernberg, L. A.; and Potter, H. G.:** Posterior tibial tendon insufficiency: which ligaments are involved? *Foot and Ankle International,* 26(6): 427-35, 2005.

13. **Sensiba, P. R.; Coffey, M. J.; Williams, I. N. E.; Mariscalco, M.; and Laughlin, R. T.:** Inter- and intraobserver reliability in the radiographic evaluation of adult flatfoot deformity. *Foot and Ankle International,* 31(2): 141-145, 2010.

14. **Younger, A. S.; Sawatzky, B.; and Dryden, P.:** Radiographic assessment of adult flatfoot. *Foot and Ankle International,* 26(10): 820-5, 2005.

15. **Saltzman, C. L., and el-Khoury, G. Y.:** The hindfoot alignment view. *Foot and Ankle International,* 16(9): 572-6, 1995.

16. **Lee, K. M.; Chung, C. Y.; Park, M. S.; Lee, S. H.; Cho, J. H.; and Choi, I. H.:** Reliability and validity of radiographic measurements in hindfoot varus and valgus. *Journal of Bone and Joint Surgery,* 92(13): 2319-2327, 2010.

17. **Perlman, P. R.; DuBois, P.; and Siskind, V.:** Validating the Process of Taking Lateral Foot X-rays. *Journal of the American Podiatry Association.,* 86(7): 317, 1996.

18. **Niki, H.; Ching, R. P.; Kiser, P.; and Sangeorzan, B. J.:** The effect of posterior tibial tendon dysfunction on hindfoot kinematics. *Foot and Ankle International,* 22(4): 292-300, 2001.

19. **Sangeorzan, B. J.; Mosca, V.; and Hansen, S. T., Jr.:** Effect of calcaneal lengthening on relationships among the hindfoot, midfoot, and forefoot. *Foot & ankle,* 14(3), 1993.

20. **Vaudreuil, N. J.; Ledoux, W. R.; Roush, G. C.; Whittaker, E. C.; and Sangeorzan, B. J.:** Comparison of Transfer Sites for Flexor Digitorum Longus in Treatment of Posterior Tibialis Tendon Dysfunction. *Journal of Bone and Joint Surgery,* In Review, 2012.

21. **Fleiss, J. L.; Levin, B.; and Paik, M. C.:** Statistical methods for rates and proportions. Edited, New York, Wiley, 1981.

22. **Arangio, G. A.; Chopra, V.; Voloshin, A.; and Salathe, E. P.:** A biomechanical analysis of the effect of lateral column lengthening calcaneal osteotomy on the flat foot. *Clinical Biomechanics,* 22(4): 472-477, 2007.

23. **Funk, D. A.; Cass, J. R.; and Johnson, K. A.:** Acquired adult flat foot secondary to posterior tibial-tendon pathology. *The Journal of bone and joint surgery. American volume,* 68(1): 95-102, 1986.

24. **Kettelkamp, D. B., and Alexander, H. H.:** Spontaneous rupture of the posterior tibial tendon. *The Journal of bone and joint surgery. American volume,* 51(4): 759-64, 1969.

25. **Johnson, K. A., and Strom, D. E.:** Tibialis posterior tendon dysfunction. *Clinical orthopaedics and related research,* (239): 196-206, 1989.

26. **Evans, D.:** Calcaneo-valgus deformity. *The Journal of bone and joint surgery. British volume,* 57(3): 270-8, 1975.

27. **Myerson, M. S.; Badekas, A.; and Schon, L. C.:** Treatment of stage II posterior tibial tendon deficiency with flexor digitorum longus tendon transfer and calcaneal osteotomy. *Foot and Ankle International,* 25(7): 445-50, 2004.

28. **Malerba, F., and De Marchi, F.:** Calcaneal Osteotomies. *Foot and Ankle Clinics,* 10(3): 523-540, 2005.

29. **Ellis, S. J.; Deyer, T.; Williams, B. R.; Yu, J. C.; Lehto, S.; Maderazo, A.; Pavlov, H.; and Deland, J. T.:** Assessment of lateral hindfoot pain in acquired flatfoot deformity using weightbearing multiplanar imaging. *Foot and Ankle International,* 31(5): 361-71, 2010.

30. **Arangio, G.; Rogman, A.; and Reed, I. J. F.:** Hindfoot alignment valgus moment arm increases in adult flatfoot with Achilles tendon contracture. *Foot and Ankle International,* 30(11): 1078-1082, 2009.

31. **Davitt, J. S.; MacWilliams, B. A.; and Armstrong, P. F.:** Plantar pressure and radiographic changes after distal calcaneal lengthening in children and adolescents. *Journal of pediatric orthopedics,* 21(1), 2001.

32. **Chi, T. D.; Toolan, B. C.; Sangeorzan, B. J.; and Hansen, S. T., Jr.:** The lateral column lengthening and medial column stabilization procedures. *Clinical orthopaedics and related research,* (365): 81-90, 1999.

33. **Oeffinger, D. J.; Pectol, R. W., Jr.; and Tylkowski, C. M.:** Foot pressure and radiographic outcome measures of lateral column lengthening for pes planovalgus deformity. *Gait & Posture,* 12(3): 189-95, 2000.

34. **Kitaoka, H. B.; Ahn, T.-K.; Luo, Z. P.; and An, K.-N.:** Stability of the Arch of the Foot. *Foot and Ankle International,* 18(10): 644, 1997.

35. **Imhauser, C. W.; Siegler, S.; Abidi, N. A.; and Frankel, D. Z.:** The effect of posterior tibialis tendon dysfunction on the plantar pressure characteristics and the kinematics of the arch and the hindfoot. *Clinical Biomechanics,* 19(2), 2004.

36. **Kim, K.-J.; Kitaoka, H. B.; Luo, Z.-P.; Ozeki, S.; Berglund, L. J.; Kaufman, K. R.; and An, K.-N.:** *In Vitro* Simulation of the Stance Phase in Human Gait. *Journal of Musculoskeletal Research,* 5(2): 113-121, 2001.

37. **Nester, C. J.; Liu, A. M.; Ward, E.; Howard, D.; Cocheba, J.; Derrick, T.; and Patterson, P.:** *In vitro* study of foot kinematics using a dynamic walking cadaver model. *Journal of Biomechanics,* 40(9): 1927-1937, 2007.

38. **Okita, N.; Meyers, S. A.; Challis, J. H.; and Sharkey, N. A.:** An objective evaluation of a segmented foot model. *Gait & Posture,* 30(1): 27-34, 2009.

39. **Hurschler, C.; Emmerich, J.; and Wülker, N.:** *In vitro* simulation of stance phase gait part I: Model verification. *Foot and Ankle International,* 24(8): 614-22, 2003.

40. **Williams, D. S., and McClay, I. S.:** Measurements used to characterize the foot and the medial longitudinal arch: reliability and validity. *Physical therapy,* 80(9): 864-71, 2000.

41. **Roush, G. C.; Whittaker, E. C.; Sangeorzan, B. J.; and Ledoux, W. R.:** Clinical Foot and Ankle X-rays with Cadaveric Specimens *Foot and Ankle International,* In Review, 2012.

42. **Whittaker, E.; Hahn, M.; Rohr, E.; Cowley, M.; Sangeorzan, B.; and Ledoux, W.:** Foot bone motion in cavus, neutral and planus feet using an *in vivo* kinematic foot model. *Gait & Posture,* In Review, 2011.

43. **De Cock, A.; De Clercq, D.; Vanrenterghem, J.; Willems, T.; and Witvrouw, E.:** The trajectory of the centre of pressure during barefoot running as a potential measure for foot function. *Gait & Posture,* 27(4): 669-675, 2008.

44. **Rosenfeld, P. F.; Dick, J.; and Saxby, T. S.:** The response of the flexor digitorum longus and posterior tibial muscles to tendon transfer and calcaneal osteotomy for stage II posterior tibial tendon dysfunction. *Foot and Ankle International,* 26(9): 671-4, 2005.

45. **Vaudreuil, N. J.; Ledoux, W. R.; Roush, G. C.; Whittaker, E. C.; and Sangeorzan, B. J.:** Comparison of transfer sites for flexor digitorum longus in treatment of posterior tibialis tendon dysfunction. *Journal of Rehabilitation,* In Review, 2012.

46. **Team, R. D. C.:** R: A language and environment for statistical computing. Edited by Computing, R. F. f. S., Vienna, Austria, 2011.

47. **Bates, D.; Maechler, M.; and Bolker, B.:** lme4: Linear mixed-effects models using S4 classes. Edited, R package version 0.999375-42, 2011.

48. **Kraszewski, A. et al.:** The Effect of Foot Type on Plantar Loading. In *Proceedings of the American Society of Biomechanics Symposium*. Edited, Providence, RI, 2010.

49. **Ellis, S. J.; Yu, J. C.; Williams, B. R.; Lee, C.; Chiu, Y. L.; and Deland, J. T.:** New radiographic parameters assessing forefoot abduction in the adult acquired flatfoot deformity. *Foot and Ankle International,* 30(12): 1168-1176, 2009.

50. **Tien, T. R.; Parks, B. G.; and Guyton, G. P.:** Plantar pressures in the forefoot after lateral column lengthening: a cadaver study comparing the Evans osteotomy and calcaneocuboid fusion. *Foot and Ankle International,* 26(7): 520-5, 2005.

51. **Benthien, R. A.; Parks, B. G.; Guyton, G. P.; and Schon, L. C.:** Lateral column calcaneal lengthening, flexor digitorum longus transfer, and opening wedge medial cuneiform osteotomy for flexible flatfoot: a biomechanical study. *Foot and Ankle International,* 28(1): 70-7, 2007.

52. **Ness, M. E.; Long, J.; Harris, G.; and Marks, R.:** Foot and ankle kinematics in patients with posterior tibial tendon dysfunction. *Gait and Posture,* 27(2): 331-339, 2008.

53. **Subotnick, S. I.:** The biomechanics of running. Implications for the prevention of foot injuries. *Sports Med,* 2(2): 144-53, 1985.

54. **Williams, D. S.; McClay, I. S.; Hamill, J.; and Buchanan, T. S.:** Lower extremity kinematic and kinetic differences in runners with high and low arches. *Journal of Applied Biomechanics,* 17(2): 153-163, 2001.

55. **Butler, R. J.; Barrios, J. A.; Royer, T.; and Davis, I. S.:** Effect of laterally wedged foot orthoses on rearfoot and hip mechanics in patients with medial knee osteoarthritis. *Prosthet Orthot Int,* 33(2): 107-16, 2009.

56. **Whittaker, E. C.; Aubin, P. M.; and Ledoux, W. R.:** Foot bone kinematics as measured in a cadaveric robotic gait simulator. *Gait Posture,* 33(4): 645-50, 2011.

57. **Okita, N.; Meyers, S. A.; Challis, J. H.; and Sharkey, N. A.:** An objective evaluation of a segmented foot model. *Gait Posture,* 30(1): 27-34, 2009.

58. R: A language and environment for statistical computing. In *R Foundation for Statistical Computing*. Edited, Vienna, Austria, R Development Core Team, 2011.

59. **McPoil, T. G., and Cornwall, M. W.:** The relationship between static lower extremity measurements and rearfoot motion during walking. *J Orthop Sports Phys Ther,* 24(5): 309-14, 1996.

60. **Nawoczenski, D. A.; Saltzman, C. L.; and Cook, T. M.:** The effect of foot structure on the three-dimensional kinematic coupling behavior of the leg and rear foot. *Phys Ther,* 78(4): 404-16, 1998.

61. **Aminian, A., and Sangeorzan, B. J.:** The anatomy of cavus foot deformity. *Foot Ankle Clin,* 13(2): 191-8, v, 2008.

62. **Ness, M. E.; Long, J.; Marks, R.; and Harris, G.:** Foot and ankle kinematics in patients with posterior tibial tendon dysfunction. *Gait & Posture,* 27(2): 331-9, 2008.

63. **Levinger, P.; Murley, G. S.; Barton, C. J.; Cotchett, M. P.; McSweeney, S. R.; and Menz, H. B.:** A comparison of foot kinematics in people with normal- and flat-arched feet using the Oxford Foot Model. *Gait Posture,* 32(4): 519-523, 2010.

64. **Nachbauer, W., and Nigg, B. M.:** Effects of arch height of the foot on ground reaction forces in running. *Med Sci Sports Exerc,* 24(11): 1264-9, 1992.